Journal of Medicinal Chemistry

ARTICLE

pubs.acs.org/jmc

Convergent Synthesis and Biological Evaluation of 2-Amino-4-(3′,4′,5′-trimethoxyphenyl)-5-aryl Thiazoles as Microtubule Targeting Agents

Romeo Romagnoli,*[,†] Pier Giovanni Baraldi,[†] Andrea Brancale,[‡] Antonio Ricci,[‡] Ernest Hamel,[§] Roberta Bortolozzi,[∥] Giuseppe Basso,[∥] and Giampietro Viola*[,∥]

[†]Dipartimento di Scienze Farmaceutiche, Università di Ferrara, 44100 Ferrara, Italy

[‡]The Welsh School of Pharmacy, Cardiff University, King Edward VII Avenue, Cardiff, CF10 3NB, U.K.

[§]Screening Technologies Branch, Developmental Therapeutics Program, Division of Cancer Treatment and Diagnosis, National Cancer Institute at Frederick, National Institutes of Health, Frederick, Maryland 21702, United States

[∥]Dipartimento di Pediatria, Laboratorio di Oncoematologia, Università di Padova, 35131 Padova, Italy

Supporting Information

ABSTRACT: Combretastatin A-4, a potent tubulin polymerization inhibitor, caused us to synthesize a novel series of 2-amino-4-(3′,4′,5′-trimethoxyphenyl)-5-aryl thiazoles with the goal of evaluating the effects of substituents on the phenyl at the 5-position of the thiazole skeleton on biological activities. An ethoxy group at the *para*-position produced the most active compound in the series, with IC_{50} values of 0.03−0.9 nM against five of seven cancer cell lines. The most active compounds retained full activity in multidrug resistant cancer cells and acted through the colchicine site of tubulin. Treated cells were arrested in the G2/M phase of the cell cycle, with cell death proceeding through an apoptotic pathway that was only partially caspase-dependent. Preliminary results suggest that, in addition to cell death by apoptosis, cells were also killed via mitotic catastrophe as an alternative cell death mechanism.

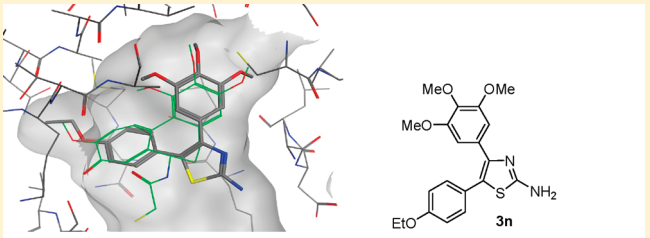

Docked pose of **3n** overlapped with DAMA-colchicine (green) in the tubulin binding-site

INTRODUCTION

The microtubule system of eukaryotic cells is a critical element in a variety of fundamental cellular processes such as cell division, formation, and maintenance of cell shape, regulation of motility, cell signaling, secretion, and intracellular transport.[1] Among the various strategies developed to block mitosis, microtubules represent an attractive target for numerous small natural and synthetic molecules that inhibit the formation of the mitotic spindle.[2] One of the most important antimitotic agents is combretastatin A-4 (CA-4, **1**; Chart 1). CA-4, isolated from the bark of the South African tree *Combretum caffrum*,[3] is one of the well-known natural molecules that strongly inhibits tubulin polymerization by binding to the colchicine site.[4] CA-4 shows potent cytotoxicity against a wide variety of human cancer cell lines, including those that are multidrug resistant,[5] and CA-4 is also a vascular disrupting agent.[6] A water-soluble disodium phosphate derivative of CA-4 (named CA-4P) has shown promising results in human cancer clinical trials,[7] thus stimulating significant interest in a variety of CA-4 analogues.[8]

Previous SAR studies have demonstrated that both the 3′,4′,5′-trimethoxy substitution pattern on the A-ring and the *cis*-olefin configuration at the bridge were fundamental requirements for optimal activity, while some B-ring structural modifications were tolerated by the target.[8,9] However, the *cis*-configuration of CA-4 is prone to isomerize to the thermodynamically more stable *trans*-form during storage and metabolism, resulting in a dramatic decrease in antitumor activity. Thus, to retain the appropriate geometry of the two adjacent aryl groups required for potent bioactivity, chemically stable *cis*-restricted derivatives of CA-4 were obtained by incorporating the olefinic double bond into vicinally diaryl-substituted five-member aromatic heterocyclic rings such as pyrazole,[10] imidazole,[11] thiazole,[12] furazan (1,2,5-oxadiazole),[13] isoxazole,[14] oxazole,[10] 1,2,3-thiadiazole,[15] triazole,[16] and 1,2,3,4-tetrazole.[12]

In a previous study, Ohsumi and co-workers reported a linear synthetic approach for the preparation of a small series of molecules based on the thiazole ring (compounds **2a**−**d**) substituted at the 2-position with a hydrogen (**2a**), methyl (**2b**), amino (**2c**), or hydrazino (**2d**) group.[12] The 2-amino derivative **2c** retains activity similar to that of CA-4 as an inhibitor of tubulin polymerization, but it is inferior to CA-4 with respect to antiproliferative activity against colon cancer cells.

Received: April 2, 2011
Published: June 13, 2011

Chart 1. Lead Structures of Tubulin Polymerization Inhibitors

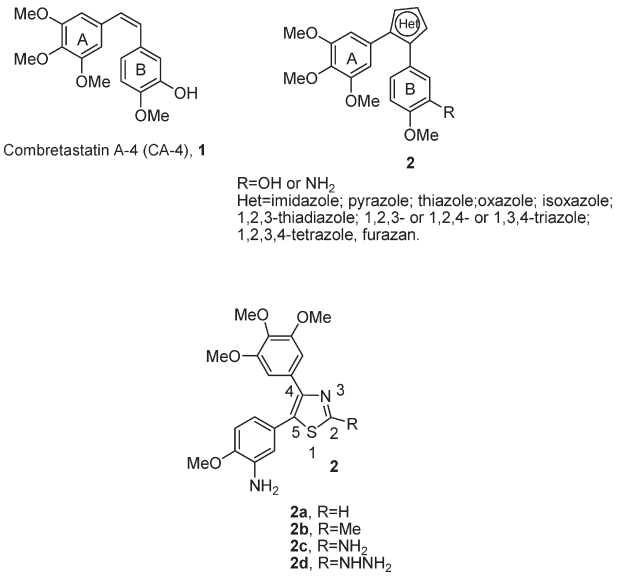

In our efforts to discover new potent antimitotic agents, we developed an efficient and versatile convergent synthetic procedure for the preparation of a new series of 2-amino-4-(3′,4′,5′-trimethoxyphenyl)-5-arylthiazoles with general structure **3**, starting from a common 2-amino protected-4-(3′,4′,5′-trimethoxyphenyl)-5-bromothiazole intermediate. In this series of designed analo- trimethoxyphenyl moiety, identical with the A-ring of CA-4, which was considered essential for maximal tubulin binding activity.[8] Modifications were focused on varying the other aryl moiety at the 5-position of the thiazole skeleton, corresponding to the B-ring of CA-4, by adding electron-withdrawing (CF_3) or electron-releasing (Me, Et, MeO, and EtO) substituents (EWG and ERG, respectively). In addition, the B-ring was replaced with naphth-1-yl, naphth-2-yl, or benzo[*b*]thienyl moieties. Because the methoxy and ethoxy groups proved to be favorable for bioactivity, we maintained one of these substituents at the *para*-position and introduced additional substituents (F, Cl, Me, and MeO) at the *meta*-position of the phenyl ring.

We examined the efficacy of the newly synthesized compounds on a panel of human cancer cell lines, including multidrug resistant lines overexpressing the 170 kDa P-glycoprotein (P-gp) drug efflux pump. Moreover, a possible mechanism of action for these compounds is described.

CHEMISTRY

The synthetic protocol employed for the preparation of 2-amino-4-(3′,4′,5′-trimethoxyphenyl)-5-aryl thiazoles **3a**−**o** is shown in Scheme 1. 2-Amino-4-(3′,4′,5′-trimethoxyphenyl)-thiazole **5** was easily obtained in good yield by the Hantzsch cyclocondensation of 2-bromo-1-(3′,4′,5′-trimethoxyphenyl)-ethanone **4** and thiourea in refluxing ethanol. The amino group was temporarily protected as the phthalimide by treatment with phthalic anhydride in refluxing acetic acid to afford **6** and then regioselectively brominated with NBS in chloroform to yield the 5-bromothiazole **7**. With our optimized conditions in hand, this latter compound was subjected to Suzuki cross-coupling conditions in the presence of the appropriate arylboronic acid under

Scheme 1[a]

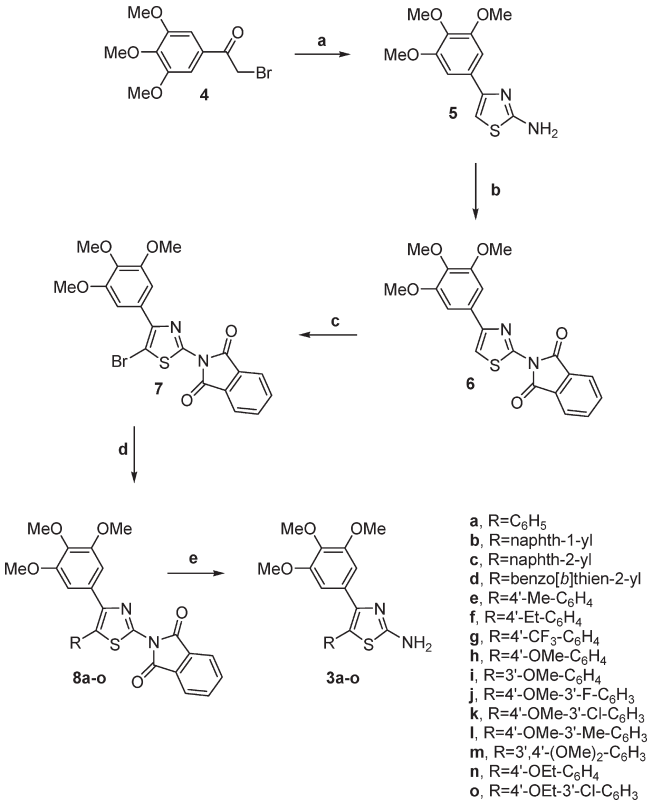

[a] Reagents. (a) thiourea, EtOH, reflux; (b) phthalic anhydride, AcOH, reflux; (c) NBS, $CHCl_3$, room temperature; (d) $PdCl_2$(DPPF), ArB-$(OH)_2$, CsF, 1,4-dioxane, 65 °C; (e) NH_2NH_2, EtOH, reflux.

heterogeneous conditions [$PdCl_2$(DPPF), CsF] in 1,4-dioxane at 65 °C to furnish derivatives **8a**−**o**.[17] The removal of the *N*-protected phthaloyl group was accomplished by the use of hydrazine in refluxing ethanol to afford final compounds **3a**−**o**.

BIOLOGICAL RESULTS AND DISCUSSION

In Vitro Antiproliferative Activities. The 2-amino-4-(3′,4′,5′-trimethoxyphenyl)-5-aryl thiazoles **3a**−**o** were evaluated for their antiproliferative activity against a panel of seven human tumor cell lines and compared with the reference compound CA-4 (**1**). The data shown in Table 1 indicated the importance of substituents on the phenyl ring at the 5-position of the thiazole system for activity and selectivity against different cancer cell lines. In general, the introduction of EWGs or ERGs increased activity compared with the unsubstituted phenyl derivative **3a**, with no clear difference in effect on potency between EWGs and ERGs. The antiproliferative activity of the most potent compounds was generally greater against the cervical carcinoma HeLa cells as compared with the other cell lines.

The 4′-ethoxyphenyl derivative **3n** displayed the strongest growth-inhibitory activity against HeLa, A549, and K562 cells, with IC_{50} values of 0.03, 0.09, and 0.07 nM, respectively. Compounds **3g** (4′-CF_3 substituent) and **3j** (4′-OMe and 3′-F substituents) were the most active molecules against MCF-7 and HT-29 cells, respectively (IC_{50}s of 0.4 and 5.7 nM, respectively). With the exception of compounds **3a**, **3b**, **3g**, **3i**, and **3m**, the tested compounds were distinctly more potent than CA-4, with

dx.doi.org/10.1021/jm200392p |*J. Med. Chem.* 2011, 54, 5144–5153

Table 1. In Vitro Cell Growth Inhibitory Effects of Compounds 3a−o and CA-4 (1)

	IC_{50}[a] (nM)						
compd	HeLa	A549	HL-60	Jurkat	K562	MCF-7	HT-29
3a	3094 ± 126	9600 ± 1490	3642 ± 132.5	3834 ± 443	8502 ± 840	>10000	7922 ± 1820
3b	3865 ± 335	6321 ± 2882	8657 ± 2403	4691 ± 325	9031 ± 891	>10000	>10000
3c	1.6 ± 0.6	3.8 ± 0.6	2.7 ± 0.3	3.3 ± 0.9	22.1 ± 7.5	51.2 ± 9.2	23.9 ± 3.9
3d	2.8 ± 0.5	16.0 ± 2.1	0.9 ± 0. 1	0.6 ± 0.01	19.6 ± 9.1	47.0 ± 2.6	19.1 ± 9.0
3e	0.73 ± 0.2	42.8 ± 5.7	3.9 ± 1.1	3.9 ± 0.6	58.7 ± 37.1	279.5 ± 69.8	12.4 ± 5.1
3f	1.0 ± 0.4	238 ± 88	1.1 ± 0.3	4.1 ± 1.1	49.7 ± 9.5	117 ± 38	54.1 ± 15.0
3g	3.2 ± 0.4	357 ± 65	5.1 ± 1.1	8.5 ± 1.2	7.6 ± 2.1	0.4 ± 0.1	221 ± 50
3h	2.3 ± 0.2	20.2 ± 1.7	3.2 ± 1.2	2.1 ± 0.4	5.1 ± 1.1	60.9 ± 8.4	11.7 ± 3.9
3i	209 ± 0.2	2374 ± 594	118 ± 30	48.4 ± 7.1	728 ± 122	476 ± 30	239 ± 44
3j	2.0 ± 0.2	3.1 ± 0.6	6.1 ± 2.1	7.3 ± 1.1	6.0 ± 2.0	18.6 ± 6.2	5.7 ± 1.5
3k	1.6 ± 0.3	37.7 ± 5.0	2.8 ± 0.4	2.9 ± 1.5	36.1 ± 18.6	27.3 ± 9.6	12.8 ± 5.0
3l	2.6 ± 0.4	305 ± 87	4.0 ± 0.3	21.5 ± 7.5	67.6 ± 28.3	58.7 ± 4.7	24.0 ± 10.4
3m	249 ± 13	1797 ± 231	301 ± 17	319 ± 80	829 ± 181	1170 ± 222	432 ± 79
3n	0.03 ± 0.005	0.09 ± 0.01	0.9 ± 0.3	0.14 ± 0.05	0.07 ± 0.004	44.0 ± 6.3	38.2 ± 11.4
3o	0.91 ± 0.32	11.2 ± 1.5	0.27 ± 0.02	0.06 ± 0.01	8.8 ± 1.0	14.1 ± 6.3	15.6 ± 7.9
CA-4	4 ± 1	180 ± 50	1 ± 0.2	5 ± 0.6	5 ± 0.1	370 ± 100	3100 ± 100

[a] IC_{50} = compound concentration required to inhibit tumor cell proliferation by 50%. Data are expressed as the mean ± SE from the dose−response curves of at least three independent experiments.

IC_{50} concentrations in the double-digit nanomolar range in the CA-4 resistant HT-29 cells. However, compound **3n** was the only compound more active than CA-4 against all cell lines.

The phenyl (**3a**) and naphth-1-yl (**3b**) derivatives were the least active compounds in the series, with IC_{50}s over 3 μM against all cell lines. Replacement of the naphth-1-yl moiety (**3b**) with the naphth-2-yl group (**3c**) resulted in a marked increase in activity, and **3c** was more active than CA-4 in five of the seven cell lines. Because the electronic properties of the **3b** and **3c** substituents are similar, the inactivity of **3b** is presumably due to steric factors caused by the naphthyl ring (see modeling section below). Replacement of the naphth-2-yl ring (**3c**) by the bioisosteric benzo[*b*]thien-2-yl moiety (**3d**) had relatively minor effects on antiproliferative activity in all cell lines.

In comparing the 4′-methylphenyl (**3e**) and 4-ethylphenyl (**3f**) with each other and with **3c** and **3d**, there were only minor differences in IC_{50} values, except that **3f** was the least active against the A549 cells and **3e** against the MCF-7 cells. Replacement of the methyl group (**3e**) with the methoxy group (**3h**) increased antiproliferative activity in five of the cell lines, with a 10-fold increase in the A549 and K562 cells.

The number and position of methoxy substituents on the C5-phenyl ring had a major influence on antiproliferative activity. Moving the methoxy group from the *para*- (**3h**) to the *meta*-position (**3i**) or the insertion of an additional methoxy group (3′,4′-dimethoxy derivative **3m**) led to a drop in potency. As noted above, the 4′-ethoxy homologue **3n** generally had the greatest antiproliferative activity of all compounds in the series. Specifically comparing it with the 4′-methoxy compound **3h**, **3n** was less active only in the HT-29 cells. The greatest differences in activity were 77-fold in the HeLa cells, 224-fold in the A549 cells, and 73-fold in K562 cells.

In comparing the effects of strong ERGs and EWGs on the phenyl at the C5 thiazole position, no consistent difference in effects on antiproliferative activity occurred. For example, replacement of the ERG methoxy group with the EWG and bulkier trifluoromethyl moiety (compounds **3h** and **3g**, respectively) resulted in an 18- and 20-fold reduction in activity against A-549 and HT-29 cells, while **3h** and **3g** showed comparable potencies against HeLa, HL-60, Jurkat, and K562 cells, but **3g** was 150-fold more active than **3h** against MCF-7 cells and was the most active compound of the series against this cancer cell line.

Relative to the activity of **3h**, the insertion of an additional EWG or ERG group on the 3′-position of the 4′-methoxyphenyl ring affected antiproliferative activity. In general, compounds **3j** and **3k**, with the EWG fluorine and chlorine atoms, showed stronger antiproliferative activities as compared with compounds with electron-releasing methyl (**3l**) and, especially, methoxy (**3m**) groups. Specific effects, however, seemed to vary with the cell line tested. Thus, with compounds **3h**−**l**, **3h** had the greatest activity with Jurkat and K562 cells, **3j** with A549, MCF-7 and HT-29 cells, and **3k** with HeLa and HL-60 cells.

Comparing the highly active 4′-ethoxy derivative **3n** with **3o**, which has an additional 3′-chloro substituent on the phenyl ring, activity was increased with **3o** by 2−20-fold against HL-60, Jurkat, MCF-7, and HT-29 cells but sharply reduced (30- to 125-fold) against HeLa, A549, and K562 cells.

Inhibition of Tubulin Polymerization and Colchicine Binding. To investigate whether the antiproliferative activities of compounds **3c**−**h**, **3j**−**l**, and **3n**−**o** derived from an interaction with tubulin, these agents were evaluated for their inhibition of tubulin polymerization and for effects on the binding of [^{3}H]colchicine to tubulin (Table 2).[18] For comparison, CA-4 was examined in contemporaneous experiments. In the assembly assay, compound **3e** was found to be the most active (IC_{50}, 0.44 μM), and it was almost 3-fold more potent than CA-4 (IC_{50}, 1.2 μM). With the exception of compounds **3d** and **3g**, all tested molecules strongly inhibited tubulin assembly, with activity superior to (**3c**, **3k**, **3n**, and **3o**) or comparable with (**3e**, **3f**, **3h**, **3j**, and **3l**) that of CA-4. Compound **3d** was half as active and **3g**, about one-fourth as active as CA-4, although **3d** and **3g** were more potent than CA-4 as antiproliferative agents against MCF-7 and HT-29 cells.

dx.doi.org/10.1021/jm200392p |*J. Med. Chem.* 2011, 54, 5144–5153

Table 2. Inhibition of Tubulin Polymerization and Colchicine Binding by Compounds 3c−h, 3j−l, 3n−o, and CA-4

compd	tubulin assembly[a] $IC_{50} \pm SD$ (μM)	colchicine binding[b] % ± SD
3c	0.74 ± 0.0	94 ± 0.7
3d	2.0 ± 0.2	86 ± 2
3e	0.44 ± 0.0	88 ± 1
3f	1.1 ± 0.0	73 ± 3
3g	4.0 ± 0.5	25 ± 0.7
3h	1.1 ± 0.0	79 ± 0.3
3j	1.2 ± 0.1	81 ± 0.2
3k	0.88 ± 0.1	77 ± 0.2
3l	1.1 ± 0.1	72 ± 3
3n	0.61 ± 0.07	95 ± 1
3o	0.89 ± 0.05	87 ± 1
CA-4 (1)	1.2 ± 0.1	98 ± 0.6

[a] Inhibition of tubulin polymerization. Tubulin was at 10 μM. [b] Inhibition of [^{3}H]colchicine binding. Tubulin, colchicine and tested compound were at 1, 5, and 5 μM, respectively.

When comparing inhibition of tubulin polymerization versus the growth inhibitory effect, we found a good correlation for most, but not all, of the active compounds. While **3e** was generally less potent than **3d** as an antiproliferative agent, **3d** was about five times less active than **3e** as inhibitor of tubulin assembly.

In the colchicine binding studies, derivatives **3c−e** and **3n−o** were almost (86−95% inhibition) as potent as CA-4, which in these experiments inhibited colchicine binding by 98%. The potent inhibition observed indicates that **3c−e** and **3n−o** bind to tubulin at a site overlapping the colchicine site. Inhibition of colchicine binding by compounds **3f**, **3h**, and **3j−l** was slightly lower (72−81%), while **3g** inhibited colchicine binding by only 25%. It is thus significant that many agents in the present series have activities superior to that of CA-4 as inhibitors of tubulin assembly and are also highly active as inhibitors of colchicine binding to tubulin.

While this group of compounds were all potent in the biological assays (inhibition of cell growth, tubulin assembly, and colchicine binding), correlations between the three assay types were imperfect. Thus, while **3e** was 5-fold more potent than **3d** in the tubulin assembly assay, these two molecules were equipotent as inhibitors of colchicine binding.

We further examined the effect of **3n**, one of the most active compounds, on the cellular microtubule network by immunofluorescence analysis. As shown in Figure 1, the microtubule network exhibited normal arrangement and organization in HeLa cells in the absence of drug treatment. In contrast, 24 or 48 h of exposure to 10 nM **3n** caused microtubule disassembly, with induction of a spherical morphology. Exposure to the compound at 100 nM resulted in an almost complete loss of microtubules. Nuclear changes were also observed. Exposure of the cells to **3n** resulted in the appearance of giant interphase cells with multiple nuclei of different sizes. In contrast to the dramatic changes in cellular microtubules, cells treated with **3n** showed minimal effects in the arrangement and amount of F-actin (Figure 1B), consistent with a preferential effect on microtubules.

Molecular Modeling. To rationalize our experimental findings, a series of molecular docking simulations on β-tubulin were performed, using a procedure reported previously.[16c] The binding

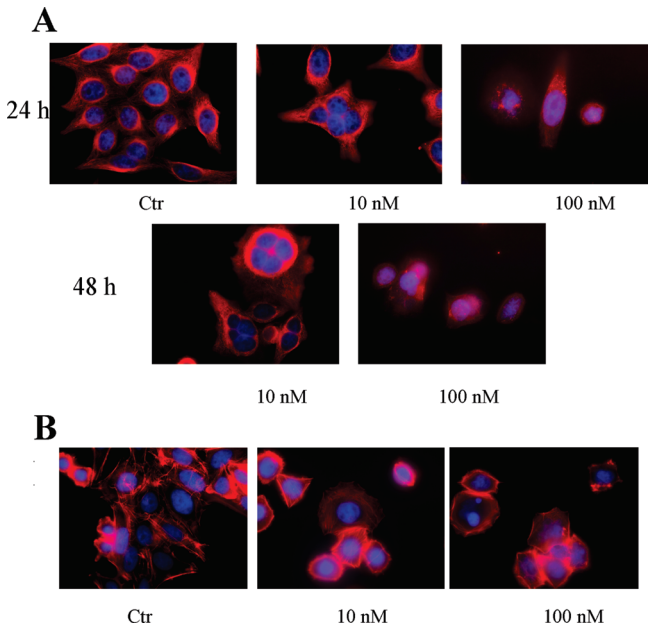

Figure 1. Immunofluorescences images of HeLa cells stained with anti-β-tubulin antibody FITC-conjugated and then observed by confocal microscopy (A). Cells were exposed to 10 or 100 nM **3n** for 24 or 48 h and then fixed and analyzed by fluorescence microscopy. Magnification 60×. (B) Representative images of HeLa cells stained with phalloidin-tetramethylrhodamine B isothiocyanate conjugate after a 24 h incubation in the presence of **3n**. Cells were also counterstained with DAPI to visualize the nuclei.

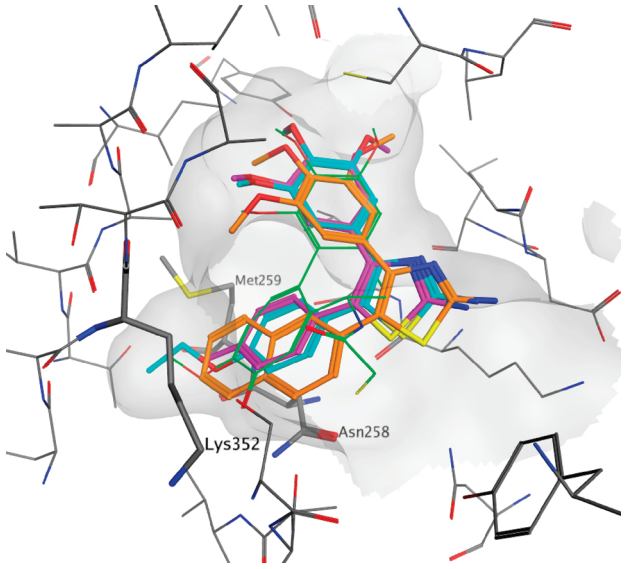

Figure 2. Docked pose of **3c** (orange), **3e** (magenta), and **3n** (cyan) overlapped with DAMA-colchicine (green) in the tubulin binding site.

mode observed for this series of compounds is very similar to the one observed for the cocrystallized DAMA-colchicine (Figure 2).[19] The trimethoxyphenyl group occupies the same position as the corresponding moiety of the colchicine analogue, while the aromatic ring in the 5 position of the thiazole ring establishes a $\pi-\pi$ interaction with Asn258 and a series of nonpolar interactions with Met259 and Lys352. Also consistent with our experimental

dx.doi.org/10.1021/jm200392p | J. Med. Chem. 2011, 54, 5144–5153

Table 3. In Vitro Cell Growth Inhibitory Effects of Compounds 3h, 3n, and 3o on Drug Resistant Cell Lines

	IC_{50}[a] (nM)					
compd	LoVo	$LoVo^{Doxo}$	CEM	CEM ^{Vbl100}	A549	A549-T12
3h	3.1 ± 1.0	0.8 ± 0.06 (0.25)[b]	7.7 ± 3.7	1.2 ± 0.6 (0.1)	20.2 ± 1.7	11.4 ± 2.3 (0.6)
3n	0.7 ± 0.08	0.6 ± 0.05 (0.9)	0.9 ± 0.2	0.8 ± 0.09 (0.9)	0.09 ± 0.01	0.2 ± 0.05 (2.2)
3o	2.0 ± 1.0	1.7 ± 0.7 (0.9)	1.4 ± 0.6	0.7 ± 0.08 (0.5)	11.2 ± 2.5	8.5 ± 1.2 (0.8)
doxorubicine	120 ± 30	13150 ± 210 (109.6)	nd	nd	nd	nd
vinblastine	nd	nd	4.1 ± 0.2	230 ± 32 (56.1)	nd	nd
taxol	nd	nd	nd	nd	7.2 ± 0.1	75.2 ± 12.5 (10.4)

[a] IC_{50} = compound concentration required to inhibit tumor cell proliferation by 50%. Data are expressed as the mean ± SE from the dose−response curves of at least three independent experiments. nd, not determined [b] Values in parentheses are fold resistance, indicating reduced potency of the compounds in the resistant cell lines

data, while the 2-naphthyl analogue **3c** binds in the way described above (Figure 2), the different orientation of the naphthyl ring of **3b** does not allow a suitable docking for this compound. Also, in the cases of compounds **3i** and **3m**, steric hindrance by the methoxy substituent in the *meta* position of the aromatic ring does not allow a successful docking, while smaller groups like F, Cl, and CH_3 in the same position (**3j**, **3k** and **3l**) can be accommodated in the binding pocket. This observation is in accordance with the experimental data obtained for these compounds as well as with the results obtained previously with another series of compounds.[16c]

Effects of Compounds 3h, 3n, and 3o on Multidrug Resistant Cell Lines. Although many anticancer drugs in clinical use are effective in the treatment of different kinds of tumors, their potential is limited by the development of drug resistance.[20] Resistance can be intrinsic or acquired but, in either case, tumors become refractory to a variety of structurally different drugs. Thus, the antiproliferative effects of **3h**, **3n**, and **3o** were evaluated in human cancer cell lines derived from a lymphoblastic leukemia ($CEM^{Vbl-100}$) and a colon carcinoma ($Lovo^{Doxo}$), both expressing high levels of the 170-kDa P-glycoprotein (P-gp) drug efflux pump.[21,22] As shown in Table 3, the examined compounds were equally potent toward parental cells and cells resistant to vinblastine or doxorubicin.

Resistance to microtubule inhibitors is also mediated by changes in the levels of expression of different β-tubulin isotypes and by tubulin gene mutations that result in modified tubulin with impaired polymerization properties. A-549-T12 is a cell line with an α-tubulin mutation with increased resistance to taxol.[23] This cell line, too, was sensitive to **3h**, **3n**, and **3o**. Thus, the data shown in Table 3 suggested that **3h**, **3n**, and **3o** might be useful in the treatment of drug refractory tumors, in particular those with resistance to other antitubulin drugs.

Analysis of Cell Cycle. The effects of different concentrations of compound **3n** on cell cycle progression were examined in HeLa and Jurkat cells (Figure 3A,B). Compound **3n** caused a clear G2/M arrest pattern in a concentration-dependent manner, starting at a concentration of 5 nM for both cell lines, a concentration higher than that which induces cytotoxicity. In parallel, we observed a concomitant decrease of cells in the G1 phase of the cell cycle (Figure 3A,B), while the percentage of S phase cells declined slightly at 100 nM for HeLa cells and extensively for Jurkat cells. Analogous behavior was also observed after 48 h of treatment (data not shown).

The apparent discrepancy between the different concentrations that induce cell cycle arrest and the cytotoxic efficacy of **3n** could be explained by the crucial role that microtubules play in maintaining normal cellular functions. Most antimitotic drugs have an all or nothing effect on cell division in the sense that they have no observable effect at low concentrations but induce a significant mitotic arrest above critical concentrations

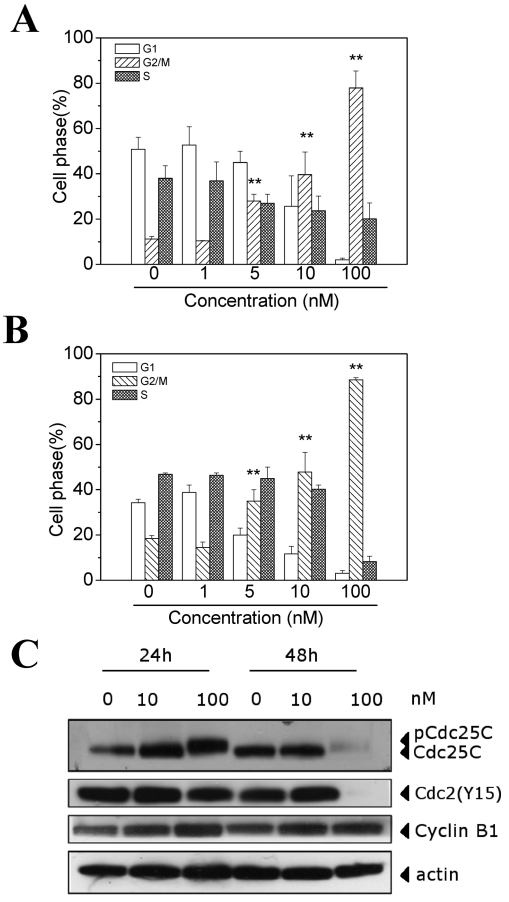

Figure 3. Effect of compound **3n** on cell cycle distribution of HeLa (A) and Jurkat cells (B). Cells were treated with different **3n** concentrations ranging from 1 to 100 nM for 24 h. Then the cells were fixed and stained with PI to analyze DNA content by flow cytometry. Data are presented as mean ± SEM of three independent experiments. ** $p < 0.01$ vs control. (C) Effect of **3n** on G2/M regulatory proteins. HeLa cells were treated for 24 or 48 h with the indicated concentration of the compound. The cells were harvested and lysed for the detection of cyclin B, p-$Cdc2^{Y15}$, and Cdc25c expression by Western blot analysis.

dx.doi.org/10.1021/jm200392p | J. Med. Chem. 2011, 54, 5144–5153

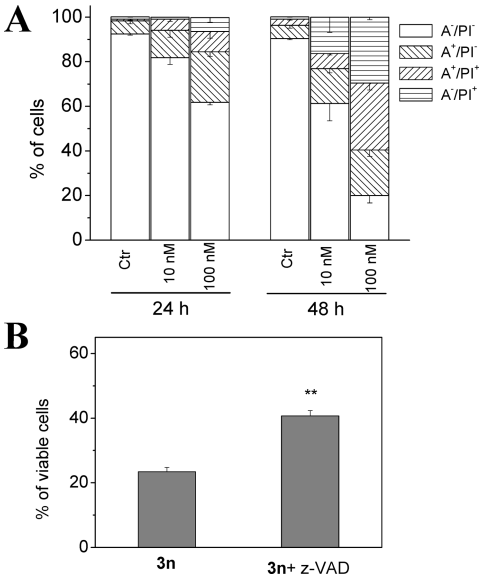

Figure 4. Flow cytometric analysis of apoptotic cells after treatment of HeLa cells with **3n**. (A) Percentage of cells found in the different regions of the biparametric histograms obtained from cytofluorimetric analysis, after incubation with **3n** for 24 or 48 h (A, annexin-V; PI, propidium iodide). (B) Percentage of cell viability after 48 h of incubation of HeLa cells with **3n** (100 nM) in the presence or in the absence of z-VAD.fmk (100 μM). Mean ± SEM of three independent experiments. $^{**}P < 0.01$ vs. **3n** treated cells.

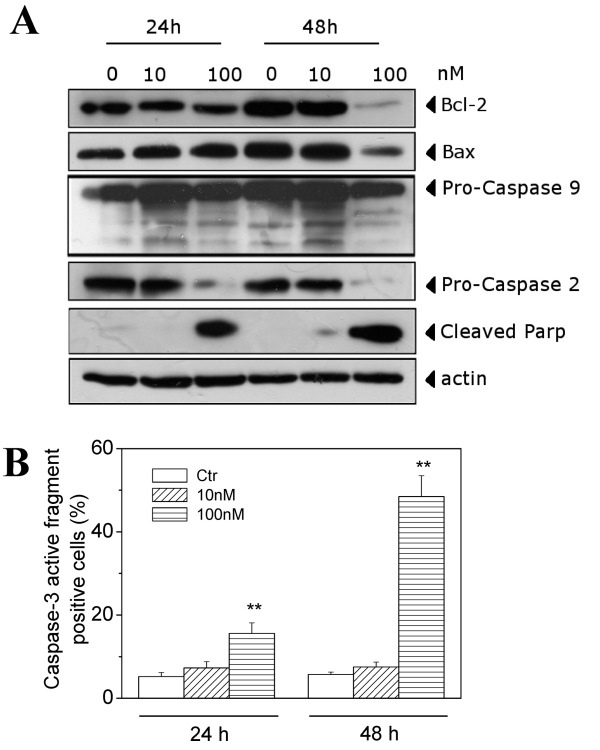

Figure 5. (A) Western blot analysis for the cleavage of PARP and the expression of Bcl-2, Bax, pro-caspase-9, and pro-caspase-2 in HeLa cells. The cells were treated with the indicated concentration of **3n** for the indicated times. Whole cell lysates were subjected to SDS-PAGE, followed by blotting with the appropriate antibody. (B) Induction of caspase-3 activity by compound **3n**. HeLa cells were incubated in the presence of **3n** at the indicated concentrations. After a 24 or 48 h treatment, cells were harvested and stained with an antihuman active caspase-3 fragment monoclonal antibody conjugated with FITC. Data are expressed as percentage of caspase-3 active fragment positive cells. ** $p < 0.01$ vs control.

and may induce cell death without an apparent block of the cell cycle.[24,25]

We next studied the association between **3n**-induced G2/M arrest and alterations in expression of proteins that regulate cell division. Cell cycle arrest at the prometaphase/metaphase to anaphase transition is normally regulated by the mitotic checkpoint.[26] In eukaryotic cells, the activation of Cdc2 kinase is necessary for occurrence of the G2/M transition of the cell cycle. Activation of the kinase requires accumulation of the cyclin B1 protein and its dephosphorylation at Tyr15 and Thr14.[26] As shown in Figure 3C in HeLa cells, **3n** caused a concentration- and time-dependent increase in cyclin B1 expression and a decreased expression of p-Cdc2^{Y15}, in particular, after 48 h of treatment.

In addition, slower migrating forms of phosphatase Cdc25c were present, especially at the concentration of 100 nM, indicating changes in the phosphorylation state of this protein. The phosphorylation of Cdc25c directly stimulates its phosphatase activity, and this is necessary to activate Cdc2/Cyclin B on entry into mitosis.[26] These results indicate that arrest at G2/M induced by **3n** is accompanied by an increased expression of cyclin B1 and, at later times (48 h) for the highest concentration (100 nM), by a marked decrease of Cdc25c and p-Cdc2^{Y15}.

Compound 3n Induces Apoptosis That Is Partially Caspase-Dependent. To characterize the mode of cell death induced by **3n**, a biparametric cytofluorimetric analysis was performed using PI, which stains DNA and is permeable only to dead cells, and fluorescent immunolabeling of the protein annexin-V, which binds to PS in a highly selective manner.[27]

Dual staining for annexin-V and with PI permits discrimination between live cells (annexin-V$^-$/PI$^-$), early apoptotic cells (annexin-V$^+$/PI$^-$), late apoptotic cells (annexin-V$^+$/PI$^+$), and necrotic cells (annexin-V$^-$/PI$^+$),[28] as shown in Figure 1s (see Supporting Information). As depicted in Figure 4A, compound **3n** at 24 h had already induced an accumulation of annexin-V positive cells in comparison with the control, and this accumulation was concentration dependent. After a 48 h incubation, we observed a further decrease of cell viability along with a marked increase in PI positive cells.

To evaluate if the cell death induced by **3n** is caspase-dependent, HeLa cells were treated with **3n** in the absence or presence of the pan-caspase inhibitor z-VAD.fmk. Inhibition of caspases significantly increased cell viability (Figure 4,B), but this caspase inhibition had only a partial impact on **3n**-induced cell death. The caspase inhibitor increased cell survival from about 20% to 40%, suggesting that other mechanism(s) may lead to cell death following treatment with **3n**.

Effect of 3n on the Activation of Caspases. To have better insight into the mechanism of cell death induced by compound **3n**, we analyzed the mitochondrial potential ($\Delta\Psi_{mt}$) after cell treatment with the compound. No changes in $\Delta\Psi_{mt}$ were observed after treatment with **3n**, as depicted in Figure 4s (see Supporting Information). We also evaluated the mitochondrial production of ROS by two fluorescent probes, HE and H_2DCFDA, by flow cytometry.[29] In agreement with the $\Delta\Psi_{mt}$ results, only a slight increase of ROS production was observed for cells treated with **3n** (Supporting Information, Figure S2).

dx.doi.org/10.1021/jm200392p | J. Med. Chem. 2011, 54, 5144–5153

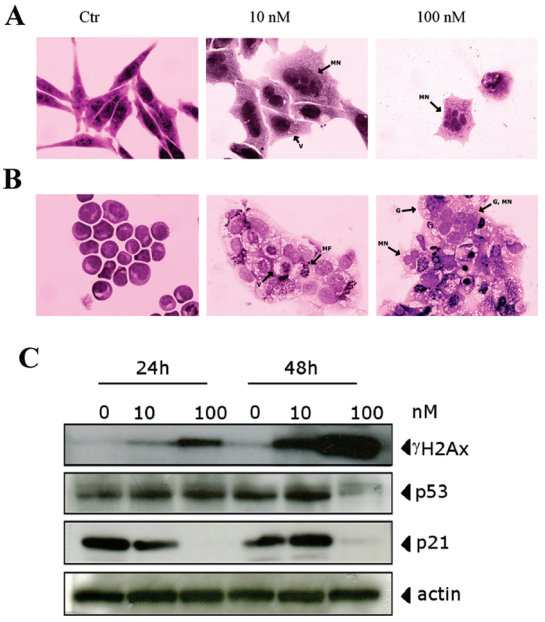

Figure 6. (A) Mitotic catastrophe. Representative images of Giemsa-stained HeLa (A) and Jurkat cells (B), observed under a light microscope after a 48 h treatment with compound **3n**. Magnification 60×. (C) Western blot analysis for the expression of p-γH2AX^{Ser139}, p53, and p21$^{waf/cip1}$ in HeLa cells. The cells were treated with the indicated concentration of **3n** for the indicated times. Whole cell lysates were subjected to SDS-PAGE, followed by blotting with the appropriate antibodies.

Next, we analyzed the effect of **3n** on the expression of two members of the Bcl-2 family, the antiapoptotic Bcl-2 and the proapototic Bax. The proteins of the Bcl family play a major role in controlling apoptosis through the regulation of mitochondrial processes and the release of mitochondrial proapoptotic molecules important for the cell death pathway.[26a] As shown in Figure 5A, **3n** did not significantly affect the expression of these two proteins at 24 h, but there was a marked decrease at 48 h following the death of a large number of cells. Altogether, these data indicate that mitochondria were not involved in the mechanism of cell death induced by **3n** at 24 h.

As shown before, apoptosis is only partially caspase-dependent. To determine which caspases were involved in **3n**-induced cell death, the expression of caspases was evaluated by immunoblot analysis and flow cytometry. We observed a clear activation in a time-dependent manner, especially at 100 nM, of the effector caspase-3 and cleavage of its substrate PARP (Figure 5A,B). Compound **3n** did not induce activation of caspase-9, the major initiator caspase of the mitochondrial apoptotic pathway (Figure 5A). Following treatment with **3n**, caspase-2 seems to be activated upstream of caspase-3. Recent evidence about the functions and activation mechanisms of the caspases indicate that caspase-2 is unique among these enzymes, displaying features of both initiator and executioner.[30] Many recent studies indicate that activation of caspase-2 is fundamental for the induction of apoptosis induced by antimitotic drugs.[31]

Compound 3n Induces Mitotic Catastrophe. It was recently demonstrated that antimitotic drugs, including CA-4, induce an alternative form of cell death to that of apoptosis. This has been called mitotic catastrophe or cell death occurring during metaphase.[32] Mitotic catastrophe is a type of cell death that usually occurs during mitosis in response to DNA damage or antimitotic agents.[33] Unlike apoptosis, which is basically dependent on caspase activation, mitotic catastrophe may be mediated in a caspase-independent or caspase-dependent fashion. In some cases, mitotic catastrophe shares the same signaling pathways with apoptosis. Cells undergoing mitotic catastrophe are characterized by multinucleation, incomplete DNA synthesis and premature chromosome condensation.[32c,d]

Morphological alterations were observed in both HeLa and Jurkat cells after 24 and 48 h of exposure to **3n** (Figure 6A,B). These changes consisted mainly of DNA condensation, abnormal mitotic figures, multinucleation, and formation of large cells. Furthermore, large cytoplasmic vacuoles were also observed in Jurkat cells.

To determine whether cell death was induced because of DNA damage, we examined the expression of phospho-γH2AX, a well-known marker for cellular DNA double-strand breaks. As shown in Figure 6C, a dramatic increase in expression of phospho-γH2AX was observed after both 24 and 48 h treatments, suggesting that DNA damage did occur after its replication was stalled by compound **3n**. In this context, p53 and p21$^{waf/cip1}$ play an essential role in inducing cell cycle arrest.[33] The p53 protein levels did not show any variation relative to the untreated cells, except at 48 h, when expression was reduced in the presence of **3n** (Figure 6C), bypassing the G2/M checkpoint stage to enter mitotic catastrophe. Cells may proceed to mitosis again by the degradation of p21. Our results showed that p21 expression was strongly reduced after both 24 and 48 h treatments with 100 nM **3n**. Downregulation of p21$^{waf/cip1}$ protein by **3n** might have contributed to the formation of multinucleated cells, as previously reported.[34]

CONCLUSIONS

An efficient convergent synthesis and biological evaluation of a new series of rigid analogues of CA-4 were described. The new compounds contain the 2-amino thiazole ring system in place of the ethylene bridge present in CA-4. We fixed one of the aryl groups as a 3′,4′,5′-trimethoxyphenyl moiety throughout the present investigation, and the modifications were mainly focused on variation of the substituents on the second aryl ring. Changes in this second aryl moiety had unpredictable effects on biological activity. The screening antiproliferative studies revealed that most of the synthesized compounds strongly inhibited the growth of all cancer cell lines examined, but specific effects were highly dependent on the aryl substituent at the 5-position of the thiazole ring, with no clear influence on activity observed by comparing the effects of ERGs and EWGs. It is clear that the substitution pattern on the phenyl moiety at the 5-position of the 2-amino thiazole ring plays an important role for antitubulin and antiproliferative activities, and this was supported by the molecular docking studies. As shown in Table 1, human cervical carcinoma HeLa cells were, in general, more sensitive toward tested compounds than the other cancer cell lines, with IC_{50} values in the low nanomolar range. Among the evaluated compounds, one of the most active analogues was found to be the 2-amino-4-(3′,4′,5′-trimethoxyphenyl)-5-(4′-ethoxyphenyl)thiazole analogue **3n**. This compound displayed antiproliferative activity at subnanomolar concentrations (IC_{50} = 0.03−0.9 nM) against all tested cancer cell lines, with the exception of HT-29 and MCF-7 cells (IC_{50} = 39 and 44 nM, respectively). Compounds **3c**−**h**, **3j**−**k**, and **3n**−**o** exhibited the strongest growth inhibition activity, with some of their IC_{50} values much lower than those

of the reference compound CA-4. More importantly, these compounds were also found to be active in cells overexpressing P-gp, suggesting that these derivatives might be useful in treating drug-refractory patients. We identified tubulin as the molecular target of all compounds examined. With most of them, tubulin polymerization was more potently inhibited than occurred with the reference compound CA-4. Like CA-4, however, all compounds inhibited colchicine binding to tubulin.

Compound **3e** was the most potent inhibitor of tubulin polymerization and one of the most potent inhibitors of colchicine binding (IC_{50} = 0.44 μM for assembly, 88% inhibition of the binding of [^{3}H]colchicine). We also showed by flow cytometry that **3n** induced apoptosis and that apoptosis induced by **3n** was only partially dependent on caspase activation. Apoptosis induced by **3n** did not involve mitochondrial depolarization. Preliminary experiments suggested that, in addition to apoptosis, cells were killed by mitotic catastrophe, as indicated by morphological changes including formation of giant cells and multinucleated cells. These observations were corroborated at the molecular level by analysis of the expression of some proteins associated with mitotic catastrophe. The ability of **3n** to induce different modes of cell death may contribute to its efficacy in different types of cancer cells, and its properties warrant its further testing in preclinical in vivo cancer models.

EXPERIMENTAL SECTION

Chemistry. Materials and Methods. ^{1}H NMR spectra were recorded on a Bruker AC 200 spectrometer. Chemical shifts (δ) are given in ppm upfield from tetramethylsilane as internal standard, and the spectra were recorded in appropriate deuterated solvents, as indicated. Positive-ion electrospray ionization (ESI) mass spectra were recorded on a double-focusing Finnigan MAT 95 instrument with BE geometry. Melting points (mp) were determined on a Buchi-Tottoli apparatus and are uncorrected. All products reported showed ^{1}H NMR spectra in agreement with the assigned structures. The purity of tested compounds was determined by combustion elemental analyses conducted by the Microanalytical Laboratory of the Chemistry Department of the University of Ferrara with a Yanagimoto MT-5 CHN recorder elemental analyzer. All tested compounds yielded data consistent with a purity of at least 95% as compared with the theoretical values. All reactions were carried out under an inert atmosphere of dry nitrogen unless otherwise indicated. Standard syringe techniques were used for transferring dry solvents. Reaction courses and product mixtures were routinely monitored by TLC on silica gel (precoated F_{254} Merck plates), and compounds were visualized with aqueous $KMnO_4$. Flash chromatography was performed using 230−400 mesh silica gel and the indicated solvent system. Organic solutions were dried over anhydrous Na_2SO_4. Arylboronic acids are commercially available and used as received. All chemicals and reagents were purchased from Aldrich (Sigma-Aldrich) or Lancaster (Alfa Aesar, Johnson Matthey Company).

Synthesis of 4-(3,4,5-Trimethoxyphenyl)thiazol-2-amine (5). The mixture of 2-bromo-1-(3,4,5-trimethoxyphenyl)ethanone (2.91 g, 10 mmol) and thiourea (836 mg, 11 mmol) in anhydrous EtOH (30 mL) was heated at reflux for 1 h. After that, the solvent was removed in vacuo, and saturated aqueous $NaHCO_3$ was added to make the mixture basic (pH = 8−9). Then the mixture was extracted with CH_2Cl_2 (3 × 25 mL). The combined organic phases were washed with brine (25 mL) and dried with anhydrous Na_2SO_4. After removal of the solvent, the residue was stirred for 20 min with petroleum ether (40 mL) and filtered to afford **5** (2.1 g, 79%) as a yellow solid, mp 170−171 °C. ^{1}H NMR ($CDCl_3$) δ: 3.86 (s, 3H), 3.92 (s, 6H), 5.42 (bs, 2H), 6.63 (s, 1H), 7.00 (s, 2H). MS (ESI): $[M]^+$ = 266.4.

Synthesis of 2-(4-(3,4,5-Trimethoxyphenyl)thiazol-2-yl)-isoindoline-1,3-dione (6). To a suspension of compound **5** (1.33 g, 5 mmol) in acetic acid (30 mL) was added phthalic anhydride (890 mg, 6 mmol). After stirring for 18 h at reflux, the solvent was evaporated and the residue dissolved in CH_2Cl_2 (50 mL). The organic solution was washed with a saturated solution of $NaHCO_3$ (15 mL), water (10 mL), and brine (10 mL), dried, and concentrated. The crude product was purified by crystallization from ethyl ether, to afford **6** (1.5 g, 76%) as a yellow solid, mp 202−203 °C. ^{1}H NMR ($CDCl_3$) δ: 3.88 (s, 3H), 3.93 (s, 6H), 7.18 (s, 2H), 7.42 (s, 1H), 7.84 (m, 2H), 8.03 (m, 2H). MS (ESI): $[M]^+$ = 396.4.

Synthesis of 2-(5-Bromo-4-(3,4,5-trimethoxyphenyl)thiazol-2-yl)isoindoline-1,3-dione (7). A solution of compound **6** (1.19 g, 3 mmol) in anhydrous chloroform (20 mL) was cooled to 0 °C and treated with NBS (746 mg, 3.3 mmol) under nitrogen. The reaction was allowed to warm to room temperature after 15 min and then stirred for 4 h. After quenching with saturated $Na_2S_2O_3$ (20 mL), the resulting mixture was diluted with water (20 mL) and extracted with CH_2Cl_2 (2 × 30 mL). The combined organics were dried ($MgSO_4$) and evaporated to give a yellow solid, which was purified by crystallization from ethyl ether, to afford **7** (1.1 g, 78%) as a yellow solid, mp 220−221 °C. ^{1}H NMR (DMSO-d_6:) δ: 3.72 (s, 3H),3.83 (s, 6H), 7.21 (s, 2H), 7.95 (m, 4H). MS (ESI): $[M]^+$ = 474.7, $[M]^+$ = 476.7

General Procedure A for the Synthesis of Compounds 8a−o. A stirred suspension of **7** (237 mg, 0.5 mmol) and the appropriate phenylboronic acid (0.75 mmol) in dioxane (6 mL containing 1 drop of water) was degassed under a stream of nitrogen over 10 min and then treated with $PdCl_2$(DPPF) (41 mg, 0.05 mmol) and CsF (190 mg, 1.25 mmol). The reaction mixture was heated under nitrogen at 45 °C for 30 min and then at 75 °C for 5 h. The reaction mixture was cooled to ambient temperature, diluted with CH_2Cl_2 (10 mL), filtered on a pad of Celite, and evaporated in vacuo. The residue was dissolved with CH_2Cl_2 (15 mL), and the resultant solution was washed sequentially with water (5 mL) and brine (5 mL). The organic layer was dried and evaporated, and the residue was purified by flash chromatography on silica gel.

General Procedure B for the Synthesis of Compounds 3a−o. A stirred suspension of a thiazole derivative (0.5 mmol) and hydrazine monohydrate (58 μL, 0.6 mmol, 1.2 equiv) in abs EtOH (10 mL) was refluxed for 1 h. The solvent was evaporated, the residue was suspended with CH_2Cl_2 (10 mL), and the suspension filtered through Celite. The filtrate was concentrated in vacuo to obtain a residue that was purified by column chromatography.

ASSOCIATED CONTENT

Supporting Information. Detailed characterization of synthesized compounds **8a−o** and **3a−o**. Experimental procedures for biological assays and computational methodology. This material is available free of charge via the Internet at http://pubs.acs.org.

AUTHOR INFORMATION

Corresponding Author

*For R.R.: phone, 39-(0)532-455303; fax, 39-(0)532-455953; E-mail, rmr@unife.it. For G.V.: phone, 39-(0)49-8211451; fax, 39-(0)49-8211462; E-mail, giampietro.viola1@unipd.it.

ACKNOWLEDGMENT

We thank Dr. Alberto Casolari for excellent technical assistance.

■ ABBREVIATIONS USED

CA-4, combretastatin A-4; EWG, electron-withdrawing group; ERG, electron-releasing group; SAR, structure−activity relationships; NBS, *N*-bromosuccinimide; $PdCl_2$(DPPF), [1,1′-bis(diphenylphosphino)-ferrocene] dichloropalladium(II) complex with dichloromethane; CsF, cesium fluoride; FITC, fluorescein isothiocyanate; PI, propidium iodide; PS, phospholipid phosphatidylserine; ROS, reactive oxygen species; HE, hydroxyethidine; H_2DCFDA, 2,7-dichlorodihydrofluorescein; PARP, poly-ADP-ribose polymerase; HBSS, Hank's Balanced Salt Solution; PBS, phosphate-buffered saline; SDS-PAGE, sodium dodecyl sulfate polyacrylamide gel electrophoresis

■ REFERENCES

(1) (a) Amos, L. A. Microtubule structure and its stabilisation. *Org. Biomol. Chem.* **2004**, *2*, 2153–2160. (b) Downing, K. H.; Nogales, E. Tubulin structure: insights into microtubule properties and functions. *Curr. Opin. Struct. Biol.* **1998**, *8*, 785–791. (c) Honore, S.; Pasquier, E.; Braguer, D. Understanding microtubule dynamics for improved cancer therapy. *Cell. Mol. Life Sci.* **2005**, *62*, 3039–3056.

(2) (a) Bhattacharyya, B.; Panda, D.; Gupta, S.; Banerjee, M. Antimitotic activity of colchicine and the structural basis for its interaction with tubulin. *Med. Res. Rev.* **2008**, *28*, 155–183. (b) Hearn, B. R.; Shaw, S. J.; Myles, D. C. Microtubule targeting agents. *Compr. Med. Chem. II* **2007**, *7*, 81–110. (c) Mahindroo, N; Liou, J. P.; Chang, J. Y.; Hsieh, H. P. Antitubulin agents for the treatment of cancer. A medicinal chemistry update. *Expert Opin. Ther. Pat.* **2006**, *16*, 647–691. (d) Jordan, M. A.; Kamath, K. How do microtubule-targeted drugs works? An overview. *Curr. Cancer Drug Targets* **2007**, *7*, 730–742. (e) Risinger, A. L.; Giles, F. J.; Mooberry, S. L. Microtubule dynamics as a target in oncology. *Cancer Treat. Rev.* **2008**, *35*, 255–261. (f) Carson, R. O. New tubulin targeting agents currently in clinical development. *Expert Opin. Invest. Drugs* **2008**, *17*, 707–722.

(3) Pettit, G. R.; Singh, S. B.; Hamel, E.; Lin, C. M.; Alberts, D. S.; Garcia-Kendall, D. Isolation and structure of the strong cell growth and tubulin inhibitor combretastatin A-4. *Experentia* **1989**, *45*, 209–211.

(4) Lin, C. M.; Ho, H. H.; Pettit, G. R.; Hamel, E. Antimitotic natural products combretastatin A-4 and combretastatin A-2: studies on the mechanism of their inhibition of the binding of colchicine to tubulin. *Biochemistry* **1989**, *28*, 6984–6991.

(5) McGown, A. T.; Fox, B. W. Differential cytotoxicity of combretastatins A1 and A4 in two daunorubucin-resistant P388 cell lines. *Cancer Chemother. Pharmacol.* **1990**, *26*, 79–81.

(6) Lippert, J. W., III. Vascular Disrupting Agents. *Bioorg. Med. Chem.* **2007**, *15*, 605–615.

(7) (a) Cooney, M. M.; Ortiz, J.; Bukowski, R. M.; Remick, S. C. Novel vascular targeting disrupting agents: combretastatin A4 phosphate and related compounds. *Curr. Oncol. Rep.* **2005**, *7*, 90–95. (b) Vincent, L.; Kermani, P.; Young, L. M.; Cheng, J.; Zhang, F.; Shido, K.; Lam, G.; Bompais-Vincent, H.; Zhu, Z.; Hicklin, D. J.; Bohlen, P.; Chaplin, D. J.; May, C.; Rafii, S. Combretastatin A4 phosphate induces rapid regression of tumor neovessels and growth through interference with vascular endothelial-cadherin signaling. *J. Clin. Invest.* **2005**, *115*, 2992–3006. (c) Chaplin, D. J.; Hill, S. A. The development of combretastatin A4 phosphate as a vascular targeting agent. *Int. J. Radiat. Oncol. Biol. Phys.* **2002**, *54*, 1491–1496. (d) Young, S. L.; Chaplin, D. J. Combretastatin A-4 phosphate: background and current clinical status. *Expert Opin. Invest. Drugs* **2004**, *13*, 1171–1182. (e) Bilenker, J. H.; Flaherty, K. T.; Rosen, M.; Davis, L.; Gallagher, M.; Stevenson, J. P.; Sun, W.; Vaughn, D.; Giantonio, B.; Zimmer, R.; Scnall, M.; O'Dwyer, P. J. Phase I trial of combretastatin A-4 phospate with carboplatin. *Clin. Cancer Res.* **2005**, *11*, 1527–1533.

(8) (a) Nam, N. H. Combretastatin A-4 analogues as antimitotic antitumor agents. *Curr. Med. Chem.* **2003**, *10*, 1697–1722. (b) Chaudari, A.; Pandeya, S. N.; Kumar, P.; Sharma, P. P.; Gupta, S.; Soni, N.; Verma, K. K.; Bhardwaj, G. Combretastain A-4 analogues as anticancer agents. *Mini Rev. Med. Chem.* **2007**, *12*, 1186–1205. (c) Tron, G. C.; Pirali, T.; Sorba, G.; Pagliai, F.; Busacca, S.; Genazzani, A. A. Medicinal chemistry of combretastatin A4: present and future directions. *J. Med. Chem.* **2006**, *49*, 3033–3044.

(9) (a) Hatanaka, T.; Fujita, K.; Ohsumi, K.; Nakagawa, R.; Fukuda, Y.; Nihei, Y.; Suga, Y.; Akiyama, Y.; Tsuji, T. Novel B-ring modified combretastatin analogues: synthesis and antineoplastic activity. *Bioorg. Med. Chem. Lett.* **1998**, *8*, 3371–3374. (b) Gaukroger, K.; Hadfield, J. A.; Lawrence, N. J.; Nlan, S.; McGown, A. T. Structural requirements for the interaction of combretastatins with tubulin: how important is the trimethoxy unit? *Org. Biomol. Chem.* **2003**, *1*, 3033–3037.

(10) Wang, L.; Woods, K. W.; Li, Q.; Barr, K. J.; McCroskey, R. W.; Hannick, S. M.; Gherke, L.; Credo, R. B.; Hui, Y.-H.; Marsh, K.; Warner, R.; Lee, J. Y.; Zielinski-Mozng, N.; Frost, D.; Rosenberg, S. H.; Sham, H. L. Potent, orally active heterocycle-based combretastatin A-4 analogues: synthesis, structure−activity relationship, pharmaokinetics, and in vivo antitumor activity evaluation. *J. Med. Chem.* **2002**, *45*, 1697–1711.

(11) (a) Schobert, R.; Biersack, B.; Dietrich, A.; Effenberger, K.; Knauer, S.; Mueller, T. 4-(3-Halo/amino-4,5-dimethoxyphenyl)-5-aryloxazoles and *N*-methylimidazoles that are cytotoxic against combretastatin A resistant tumor cells and vascular disrupting in a cisplatin resistant germ cell tumor model. *J. Med. Chem.* **2010**, *53*, 6595–66002. (b) Bonezzi, K.; Taraboletti, G.; Borsotti, P.; Bellina, F.; Rossi, R.; Giavazzi, R. Vascular disrupting activity of tubulin-binding 1,5-diaryl-1*H*-imidazoles. *J. Med. Chem.* **2009**, *52*, 7906–7910.

(12) Ohsumi, K.; Hatanaka, T.; Fujita, K.; Nakagawa, R.; Fukuda, Y.; Nihai, Y.; Suga, Y.; Morinaga, Y.; Akiyama, Y.; Tsuji, T. Synthesis and antitumor activity of cis-restricted combretastatins 5-membered heterocyclic analogues. *Bioorg. Med. Chem. Lett.* **1988**, *8*, 3153–3158.

(13) Tron, G. C.; Pagliai, F.; Sel Grosso, E.; Genazzani, A. A.; Sorba, G. Synthesis and cytotoxic evaluation of combretafurazans. *J. Med. Chem.* **2005**, *48*, 3260–3258.

(14) Liu, T.; Dong, X.; Xue, N.; Wu, R.; He, Q.; Yang, B.; Hu, Y. Synthesis and biological evaluation of 3,4-biaryl-5-aminoisoxazole derivatives. *Bioorg. Med. Chem.* **2009**, *17*, 6279–6285.

(15) Wu, M.; Li, W.; Yang, C.; Chen, D.; Ding, J.; Chen, Y.; Lin, L.; Xie, Y. Synthesis and activity of combretastatin A-4 analogues: 1,2,3-thiadiazoles as potent antitumor agents. *Bioorg. Med. Chem. Lett.* **2007**, *17*, 869–873.

(16) (a) Odlo, K.; Hentzen, J.; Fournier dit Chabert, J.; Ducki, S.; Gani, A. B. S. M. O.; Sylte, I.; Skrede, M.; Florenes, V. A.; Hansen, T. V. 1,5-Disubstituted 1,2,3-triazoles as cis-restricted analogues of combretastatin A-4: synthesis, molecular modeling and evaluation as cytotoxic agents and inhibitors of tubulin. *Bioorg. Med. Chem.* **2008**, *16*, 4829–4838. (b) Zhang, Q.; Peng, Y.; Wang, X. I.; Keeman, S. M.; Aurora., S.; Welsh, W. J. Highly potent triazole-based tubulin polymerization inhibitors. *J. Med. Chem.* **2007**, *50*, 749–754. (c) Romagnoli, R.; Baraldi, P. G.; Cruz-Lopez, O.; Lopez-Cara, C.; Carrion, M. D.; Brancale, A.; Hamel, E.; Chen, L.; Bortolozzi, R.; Basso, G.; Viola, G. Synthesis and antitumor activity of 1,5-disubstituted 1,2,4-triazoles as cis-restricted combretastatin analogs. *J. Med. Chem.* **2010**, *53*, 4248–4258.

(17) For a general review on palladium cross-coupling reactions see: Miyaura, N.; Suzuki, A. Palladium-catalyzed cross-coupling reactions of organoboron compounds. *Chem. Rev.* **1995**, *95*, 2457–2483.

(18) (a) Hamel, E. Evaluation of antimitotic agents by quantitative comparisons of their effects on the polymerization of purified tubulin. *Cell Biochem. Biophys.* **2003**, *38*, 1–21. (b) Verdier-Pinard, P.; Lai, J.-Y.; Yoo, H.-D.; Yu, J.; Marquez, B.; Nagle, D. G.; Nambu, M.; White, J. D.; Falck, J. R.; Gerwick, W. H.; Day, B. W.; Hamel, E. Structure−activity analysis of the interaction of curacin A, the potent colchicine site antimitotic agent, with tubulin and effects of analogs on the growth of MCF-7 breast cancer cells. *Mol. Pharmacol.* **1998**, *53*, 62–67.

(19) Ravelli, R. B. G.; Gigant, B.; Curmi, P. A.; Jourdain, I.; Lachkar, S.; Sobel, A.; Knossow, M. Insight into tubulin regulation from a complex with colchicine and a stathmin-like domain. *Nature* **2004**, *428*, 198–202.

(20) Baguley, B. C. Multidrug resistance mechanism in cancer. *Mol. Biotechnol.* **2010**, *46*, 308–316.
(21) Dupuis, M.; Flego, M.; Molinari, A.; Cianfriglia, M. Saquinavir induces stable and functional expression of the multidrug transporter P-glycoprotein in human CD4 T-lymphoblastoid CEM rev cells. *HIV Med.* **2003**, *4*, 338–345.
(22) Toffoli, G.; Viel, A.; Tuimoto, I.; Bisconti, G.; Rossi, G.; Baoiocchi, M. Pleiotropic-resistant phenotype is a multifactorial phenomenon in human colon carcinoma cell lines. *Br. J. Cancer* **1991**, *63*, 51–56.
(23) Martello, L. A.; Verdier-Pinard, P.; Shen, H. J.; He, L.; Torres, K.; Orr, G. A.; Horwitz, S. B. Elevated level of microtubule destabilizing factors in a taxol-resistant/ dependent A549 cell line with an alpha-tubulin mutation. *Cancer Res.* **2003**, *63*, 448–454.
(24) Chen, J. G.; Horwitz, S. B. Differential mitotic responses to microtubule-stabilizing and -destabilizing drugs. *Cancer Res.* **2002**, *62*, 1935–1938.
(25) Gascoigne, K. E.; Taylor, S. S. Cancer cells display profound intra and interline variation following prolonged exposure to antimitotic drugs. *Cancer Cell* **2008**, *14*, 111–122.
(26) (a) Mollinedo, F.; Gajate, C. Microtubules, microtubule-interfering agents and apoptosis. *Apoptosis* **2003**, *8*, 413–450. (b) Clarke, P. R.; Allan, L. A. Cell-cycle control in the face of damage—a matter of life or death. *Trends Cell Biol.* **2009**, *19*, 89–98.
(27) Vermes, I.; Haanen, C.; Steffens-Nakken, H.; Reutelingsperger, C. A novel assay for apoptosis. Flow cytometric detection of phosphatidylserine expression on early apoptotic cells using fluorescein labelled annexin V. *J. Immunol. Methods* **1995**, *184*, 39–51.
(28) Martin, S. J.; Reutelingsperger, C. P.; McGahon, A. J.; Rader, J. A.; van Schie, R. C.; Laface, D. M.; Green, D. R. Early redistribution of plasma membrane phosphatidylserine is a general feature of apoptosis regardless of the initiating stimulus: inhibition by overexpression of Bcl-2 and Abl. *J. Exp. Med.* **1995**, *182*, 1545–1556.
(29) (a) Rothe, G.; Valet, G. Flow cytometric analysis of respiratory burst activity in phagocytes with hydroethidine and 2′,7′-dichlorofluorescein. *J. Leukocyte Biol.* **1990**, *47*, 440–448. (b) Cai, J.; Jones, D. P. Superoxide in apoptosis. Mitochondrial generation triggered by cytochrome *c* loss. *J. Biol. Chem.* **1998**, *273*, 11401–11404. (c) Nohl, H.; Gille, L.; Staniek, K. Intracellular generation of reactive oxygen species by mitochondria. *Biochem. Pharmacol.* **2005**, *69*, 719–723.
(30) Vakifahmetoglu-Norberg, H.; Zhivotovsky, B. The unpredictable caspase-2: what can it do? *Trends Cell Biol* **2010**, *20*, 150–159.
(31) (a) Mhaidat, N. M.; Wang, Y.; Kiejda, K. A.; Zang, X. D.; Hersey, P. Docetaxel-induced apoptosis in melanoma cells is dependent on activation of caspase-2. *Mol. Cancer Ther.* **2007**, *6*, 752–761. (b) Ho, L. H.; Read, S. H.; Dorstyn, L.; Lambrusco, L.; Kumar, S. Caspase-2 is required for cell death induced by cytosketal disruption. *Oncogene* **2008**, *27*, 3393–3404.
(32) (a) Vitale, I.; Antoccia, A.; Cenciarelli, C.; Crateri, P.; Meschini, S.; Arancia, G.; Pisano, C.; Tanzarella, C. Combretastatin A-4 and combretastatin derivative induce mitotic catastrophe dependent on spindle checkpoint and caspase-3 activation in non-small cell lung cancer cells. *Apoptosis* **2007**, *12*, 155–166. (b) Cenciarelli, C.; Tanzarella, C.; Vitale, I.; Pisano, C.; Crateri, P.; Meschini., S.; Arancia, G.; Antoccia, A. The tubulin-depolymerising agent combretastatin-4 induces ectopic aster assembly and mitotic catastrophe in lung cancer cells H460. *Apoptosis* **2008**, *13*, 659–669. (c) Castedo, M.; Perfettini, J. L.; Roumier, T.; Andreau, K.; Medema, R.; Kroemer, G. Cell death by mitotic catastrophe: a molecular definition. *Oncogene* **2004**, *23*, 2825–2837. (d) Vakifahmetoglu, H.; Olsson, M.; Zhivotovsky, B. Death trough a tragedy: mitotic catastrophe. *Cell Death Differ.* **2008**, *15*, 1153–1162.
(33) Portugal, J.; Mansilla, S.; Bataller, M. Mechanisms of drug-induced mitotic catastrophe in cancer cells. *Curr. Pharm Des.* **2010**, *16*, 69–78.
(34) Mantel, C.; Braun, S. E.; Reid, S.; Henegariu, O.; Liu, L.; Hangoc, G.; Broxmeyer, H. E. p21(cip^1/waf^1) deficiency causes deformed nuclear architecture, centriole overduplication, polyploidy, and relaxed microtubule damage checkpoints in human hematopoietic cells. *Blood* **1999**, *15*, 1390–1398.